AIAA JOURNAL
Vol. 46, No. 7, July 2008

Study of Damping Linearity of Jointed Metal Plates

Scott J. I. Walker* and Guglielmo S. Aglietti†
University of Southampton,
Southampton, England SO17 1BJ, United Kingdom
and
Paul Cunningham‡
University of Loughborough,
Leicestershire, England LE11 3TU, United Kingdom

DOI: 10.2514/1.34323

Dynamic models are widely used in many branches of science and engineering, and it has been argued that many of the shortfalls with these models are due to the fact that the physics of joint dynamics are not fully understood. This makes the phenomenon very hard to model theoretically from first principles. Experimental analyses are therefore widely used to underpin any work in this area. This study aims to build on the previous experimental work based on simple beam joints and analyzes the damping trends for metal panels. This incorporates torsional effects into the system creating more complex displacements of the joint. Five panel configurations are investigated using an experimental approach that minimizes all external influences on the dynamics of the panels. Each mode loss factor is determined from these experimental tests and compared with the most established theoretical model in the field. The corresponding joint displacements and decay trends are also analyzed, producing indications as to the likely dominant source of damping, suggesting that the mode shapes can be categorized based on their displacement and dominant damping source.

Nomenclature

E = Young's modulus of elasticity
ρ = density

I. Introduction

IN THE current world of engineering, structural vibration problems continue to impact the design and construction of a wide range of products. The dynamics and sound transmission characteristics of structures are determined by essentially three parameters: mass, stiffness, and damping [1]. Damping controls the amplitude of the structural response at resonance and is responsible for the eventual decay of the free vibrations in any system and, as such, it is an important parameter to determine when attempting to predict the dynamic behavior of a structure. To this day, damping is still the dynamic characteristic that is least understood and the most difficult to quantify. The prediction of damping is particularly challenging for built-up structures due to the limited knowledge of how joints affect the damping of the complete structure. This is true not only in terms of the approximate damping magnitude but also the trends and linearity of the damping decay. It is therefore necessary to experimentally analyze a range of structural joints to investigate both magnitude and decay trends in an initial step to building up the structural complexity of the system.

To date, decades of research in this area have produced a great wealth of knowledge. However, due to the many detailed damping mechanisms inherent in structural joints, it remains an area of considerable research activity [2–4]. The two main mechanisms that are commonly referred to are air pumping and friction. Various works have been performed to study these two mechanisms [5,6], but the knowledge is not extensive enough to be generally applied with any accuracy. The most in-depth analysis performed in the 1960s [6] identified air pumping to be the dominant source of damping in structural joints and quantified the damping based on empirical data for a range of joint parameters, such as joint width, length, fastener spacing, material, and air pressure. However, this investigation and theoretical approach was focused on high-frequency vibration of a single line of tight fasteners. More recent work has been performed to investigate the effect of the joint variables [7,8]. However, in analyzing the effect of a single variable, the remaining variables have to be constant, therefore the results are very specific to the nature of the constant parameters, the experimental approach, and the procedure. In fact, it has even been stated that "little can be done to control or estimate the magnitude of joint damping or even to identify the dominant source within the joint" [9]. A simple but effective investigation into air pumping performed by Wylie (1998 [10]) measured the damping magnitude from a simple small beam joint in air and a vacuum. It concluded that air pumping contributed to as much as half the modal damping magnitude. Many derived damping models have been based around simple joint experiments on single- or double-bolted beamlike specimens [11–15]. However, these neglect torsional effects on the joint. An added complication of panel joints is the increased material area and the consequential damping effect of the whole vibrating panel. It has been previously stated [9] that, at low frequencies, this source of damping can be the predominant source of plate damping, an effect that can be enhanced by added stiffeners. It is known from the simple beam experiments in [11] that the location of the joint has an effect on the damping due to the modal curvature at the joint location. A high curvature across the joint increased the damping magnitude as a result of the increased effect of air pumping at the joint interface. This phenomenon is likely to be present for jointed panels but will be made more complex with the addition of torsional displacements along the joint edge. The damping and vibration of jointed metal panels have been investigated previously [16], but these tests have incorporated constraining, passive damping, and excitation methods that inherently affect the true damping properties of the free panel. For example, Deraemaeker et al. [17] use a test method that constrains and excites a jointed panel in a way that minimizes torsional displacements. This present study

Received 6 September 2007; revision received 21 February 2008; accepted for publication 3 March 2008.

*Lecturer, Astronautics Research Group, School of Engineering Sciences.
†Senior Lecturer in Aerospace Structural Dynamics, School of Engineering Sciences.
‡Lecturer in Advanced Aerospace Materials and Structures, Aeronautical and Automotive Engineering.

aims to experimentally investigate the damping linearity and magnitude of bolted and riveted metal panels using a test method that minimizes any external influence on the natural free vibration of the panel.

II. Experimental Approach

An experimental test campaign was carried out with the aim of measuring the damping of jointed panels and comparing these values to an equivalent monolithic panel.

A. Test Specimens

The test panels were sized to be large enough to have a significant mass but small enough to be manageable for testing. It was also desirable to avoid square panels, reducing the likelihood of unusual symmetrical modes. Therefore, the ratio of length to height was chosen to be around 0.7. All the panels were cut from a single sheet of 6082-T6 aluminium with a thickness of 2 mm ($E = 70 \times 10^9$ N · m^{-2}, $\rho = 2700$ kg · m^{-3}). The exact dimensions of the panels are displayed in Fig. 1.

Two jointed panels were constructed to allow the effect of two different types of fasteners to be investigated, namely, bolts and rivets. The location and spacing of the fasteners were identical for both jointed panel configurations forming two lines with a separation distance of 30 mm. Seventeen fasteners were used in each configuration and were staggered as shown in Fig. 2.

The three panel configurations were denoted as A, B, and C for the monolithic, bolted, and riveted panels, respectively. To determine the impact of the joint stiffness on the damping of the panel, configuration B was tested at three different bolt torque magnitudes, 1.5, 3, and 4.5 N · m. This resulted in a total of five panel variations that would be subjected to experimental testing. A summary of these panel configurations can be seen in Table 1.

B. Initial Test Procedure

Experimental tests were performed to determine the loss factors for the first 12 modes of each configuration (up to around 170 Hz) and to identify the mode shapes and their respective frequencies. The first 12 modes were selected, as these included all the basic bending and torsion modes and also allowed a comparison between these lower modes and equivalent higher mode shapes.

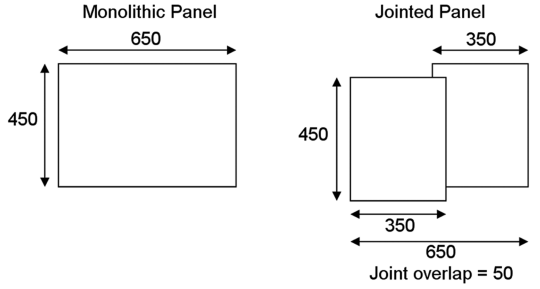

Fig. 1 Experimental panel layout (not to scale, all dimensions in millimeters).

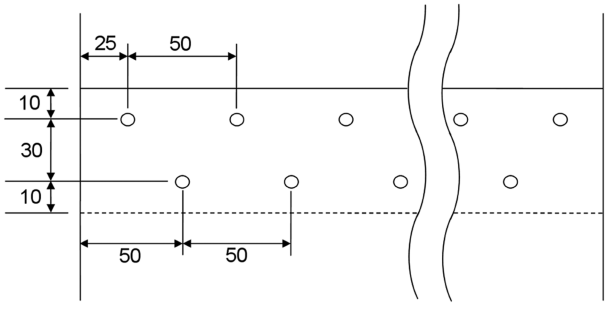

Fig. 2 Joint parameters (not to scale, all dimensions in millimeters).

Table 1 Summary of test configurations

Configuration	Properties	Variations
A	Monolithic plate	None
B	Bolted joint	Bolt torque: 1.5, 3, 4.5 N · m
C	Riveted joint	None

The first 12 mode shapes are displayed in Fig. 3, theoretically determined using finite element simulations in ANSYS 7.1.

For the first set of tests, the panels were suspended from two fixed mounting points and excited using a pendulum-mounted impact hammer, allowing high accuracy in the position of the excitation and repeatability [8]. The resultant accelerations were measured using miniature teardrop-shaped accelerometers with a mass of 0.6 g each. These items are shown in Fig. 4.

The signals from the accelerometers were captured on a computer at a sample rate of 5000 Hz. Each vibration response was analyzed using a sonogram, which is a time-varying spectrum calculated from time series data by Fourier analysis. The decay rate was subsequently computed by using a linear regression of the variation of logarithmic amplitude with time. This analysis was performed in MATLAB 7.0.1 using a code developed by Hodges et al. [18]. The decay results for each mode were averaged, allowing the standard deviation of the data to be determined. The linearity of the damping with respect to the decibel reduction over time was quantified using RSQ (R squared) values, which is the square of the Pearson product moment correlation coefficient [19]. The closer this value is to one, the more linear the logarithmic decay result.

Initial tests were performed using both wax- and glue-mounted accelerometers and, as anticipated, it was found that, for this frequency range, the method of accelerometer mounting had no significant effect on the measured damping magnitude. Wax was therefore used throughout the testing campaign, as the accelerometers had to be frequently moved between the mounting points.

These preliminary tests allowed initial correlations to be made between the mode shapes and their respective frequencies, but highlighted the effects of the external influences on the damping of the panels.

C. External Influences on Dynamics of the Panel

As the modal loss factors for metal plates (and especially aluminum plates) are known to be so low [1], any external influence on the panel's vibration will noticeably affect the damping of the panel and therefore the accuracy of the data. For vibration testing using an impact hammer, the external damping influence primarily comes from two sources: the support mounting of the panel and any added mass/attachments on the panel, i.e., accelerometers.

To perform vibration tests on configurations A–C, the panels were initially suspended from two fixed points located along the larger panel edge. However, it was found that, as expected for certain mode shapes, this resulted in a large loss factor variability as the mounting points were being excited and therefore created another source of damping of the panel. To overcome this problem, the panels were mounted from the nodal points of each mode shape, minimizing the excitation of the mounting locations. When the variable mounting loss factor magnitudes were compared with the fixed mounting results [20], it was shown that the loss factor variability and magnitude increased for the mode shapes that excite the longer panel edge (i.e., mode shapes one and four). For the remaining mode shapes, the loss factor change was insignificant displaying the consistency of the data. The corresponding increase in the reliability of the data was also shown using the RSQ values. The fixed and variable mounting tests have average RSQ values over the first eight modes of 0.940 and 0.995, respectively. Therefore, as anticipated, the variable mounting condition is the most accurate method for determining the loss factors, a trend found not only from the decay

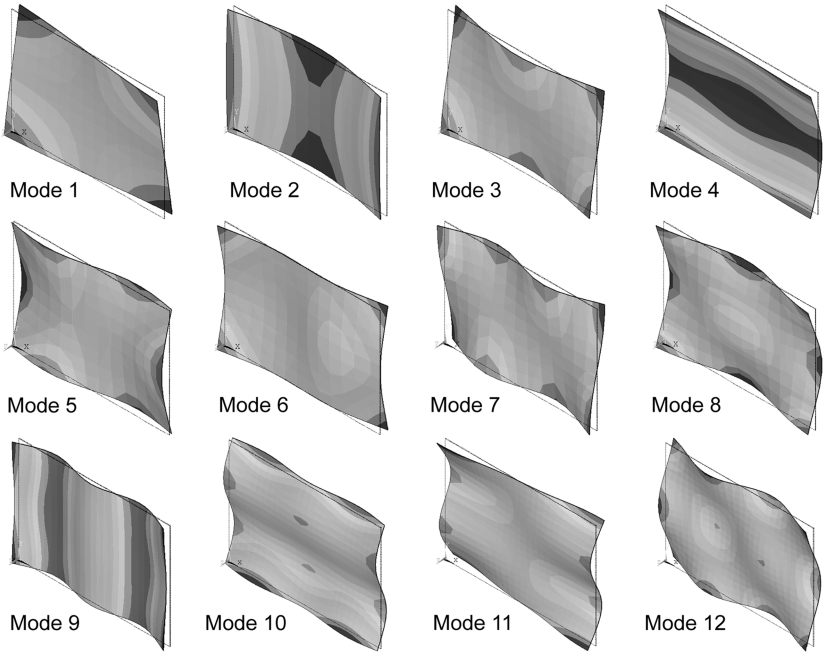

Fig. 3 General mode shapes 1–12.

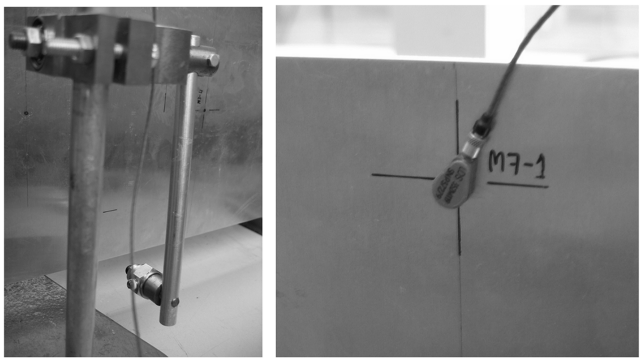

a) **b)**

Fig. 4 Pendulum mounted impact hammer and teardrop accelerometer.

data but also from the average RSQ values. However, the variable mounting test method is the most time consuming as every panel must be suspended using different mounting points for every mode and configuration. From the point of view of the general application of this approach, it is also limited to panels that enable the complete flexibility required to suspend the specimen from any location.

From the initial tests performed, it was found that even the miniature accelerometers and connection cables had a noticeable influence on the damping magnitude when used in sufficient numbers. Four accelerometers were being used in the initial test case. It was therefore decided to use a single accelerometer to minimize this effect.

D. Test Setup

Having correlated the mode shapes with their respective frequencies, these were validated using simple exploratory analyses, moving the accelerometer to predicted node and antinode locations for each mode. Having matched each mode shape to its correct frequency, the panels were marked out to set the nodal mounting positions, accelerometer locations, and excitation positions. To minimize the excitation of two modes at a similar frequency, the accelerometer and excitation positions were carefully selected to excite and record vibration data for only one of these mode shapes. For example, to get a clear signal for frequency "A," you can minimize frequency "B" response from the data by exciting along a nodal line of frequency "B." The experimental setup for mode 7, configuration A can be seen in Fig. 5.

For each panel and mode under test, four accelerometer positions were used, taking six and seven signals from each position to total 25 damping values for each mode. The excitation position for each mode remained the same as the accelerometer was moved. Data comparisons were performed to attempt to identify any correlation between accelerometer location and damping decay result. However, no consistent trends were found.

Twenty-five damping values were recorded, per mode, per configuration, resulting in 1500 hammer hits to obtain the complete data set. It is clear that this detailed level of testing could not easily be applied to many practical test cases. However, the aim of this paper is to identify linearity trends from the best quality data and to link these trends with the mode shapes.

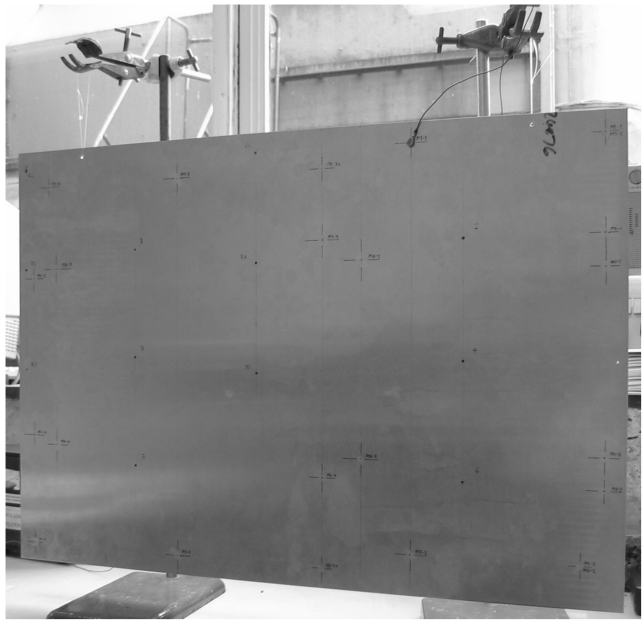

Fig. 5 Experimental setup for mode 7, configuration A.

IV. Comparative Models

Equivalent finite element models were constructed using ANSYS 7.1 to give comparative results for the resonant frequencies, the mode shapes, and the nodal displacements patterns. The models were created using SHELL63 and SHELL91 elements for the monolithic and jointed panels, respectively [21]. An element size of 25 mm was used for the monolithic simulation. The number of elements was increased for the jointed model (using an element size of 10 mm) to increase the number of possible constraints along the width and length of the joint.

Initial trial simulations were performed using contact elements to simulate the plate joints. However, this form of modeling does not allow a linear solution (i.e., a modal analysis), significantly increasing the difficulty in obtaining the modal solution of the problem. It can also be a significant challenge to simulate the modal displacement accurately, especially for the higher modes. Therefore, as these models were only intended to be an approximate guide, more simplistic simulations were run. These were performed on two different models, the first of which incorporated a joint where all the nodes were merged. The second incorporated a joint where half the nodes were merged together. These simulations produced initial resonant frequency estimates along with their corresponding mode shapes, and identified seven resonant frequencies below 100 Hz, equivalent to the experimental results. It was found for the monolithic panel that, in general, the theoretical values corresponded well with the experimental results, within an error of 5%. The main discrepancies were caused by the experimental mounting supports, and when these were included in the theoretical model, the errors reduced to within 5%. For the jointed panel, the most consistently accurate model was found to be the half-merged joint with an average errors value of less than 8%. It was found from this model that all the mode shapes were equivalent to the monolithic case, except for order changes for modes 12 and 13. Although mode 13 is beyond the scope of this investigation, this mode shape order change is important to take into account when comparing the damping data.

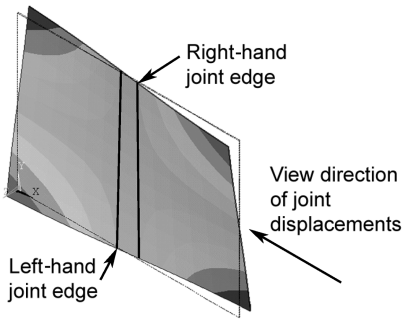

Fig. 6 View direction of joint displacements.

As it has been identified that the damping due to air pumping can be as much as half the modal damping magnitude [10], a displacement analysis was performed along the edges of the joint. The aim of this analysis was to identify which mode shapes caused the joint to open, resulting in an increase in the effect of air pumping. The displacements of the monolithic panel along the joint edge positions were output from ANSYS and plotted from the view direction shown in Fig. 6. The joint edge displacements for all of the first 12 modes are displayed in Fig. 7.

When these displacement data are viewed alongside Fig. 3, certain modal trends can be found, grouping the mode shapes together in relation to how these displacements affect the joint. First, modes 1, 7, and, to a lesser extent, 11 and 12, all display sharp opposing displacements across the joint. Modes 1 and 7 are torsional displacements across the joint, whereas the displacements from modes 11 and 12 result from more complex bending modes. However, the general displacement trend across the joint groups these modes together, to be defined as "cross" modes. The next group that can be defined results from longitudinal bending modes that displace the whole joint away from the *y* axis, creating a curvature across the joint (a trend which has a notable impact on the damping magnitude of the joint, as shown in [11]). This group comprises

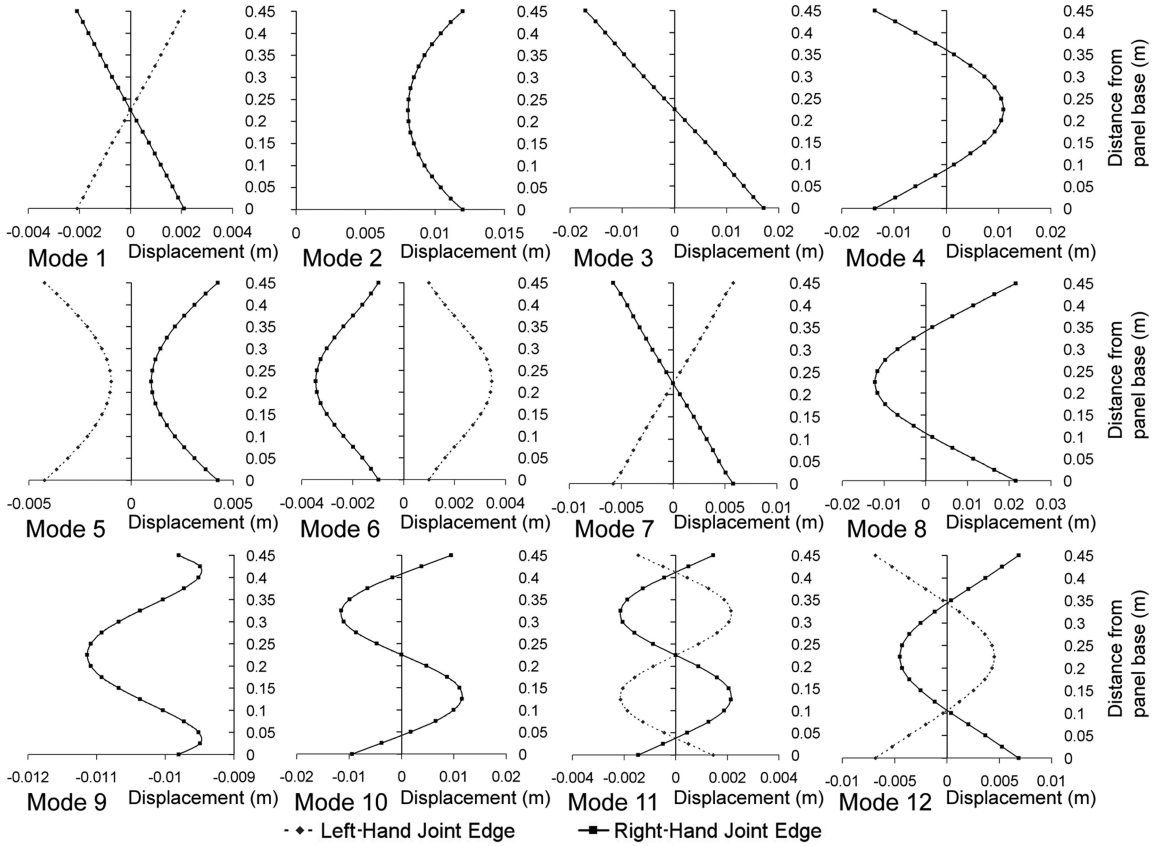

Fig. 7 Simulated joint edge displacements.

modes 2 and 9, which are defined as the "longitudinal bending" modes. The corresponding "transverse bending" group consists of modes 4, 8, and 10. The trends of these displacements are that both joint edges displace together and cross the vertical y axis creating the transverse curvature. The remaining modes are more unique and, for the purposes of this investigation, will be defined as "variable" modes. These modes are 3, 5, and 6. It is now necessary to analyze the effect of these joint displacements in terms of the modal damping magnitude and the linearity of the damping.

V. Experimental Test Results

As stated previously, the vibration response from each experimental test was analyzed using a sonogram, which plots time against frequency as a contour plot, where the out-of-plane dimension is the vibration amplitude (Fig. 8a).

Each resonant frequency identified in the contour plot can be analyzed further to display the decay trend for each mode over whichever time period of the decay is selected, as displayed in Fig. 8b. Therefore, for nonlinear decays (with respect to the decibel decay over time), the straight line approximation is highly dependent on which time period of the decay is selected. For the example shown in Fig. 8b, the initial decay gradient over the first second was used for the average loss factor analysis, as this is the most severe damping case. It could be argued that a linear interpolation may not be the best simulation of this system. However, it is the aim of this study to determine the linearity and applicability of these logarithmic decays. All other more linear decibel decays were measured over the maximum time length possible to create representative averages for the data. The complete set of the average experimental damping decay magnitudes is shown in Fig. 9 [8], alongside theoretical air-pumping damping results calculated using the approach outlined by Ungar [22]. This approach is based on empirical data of a single line of fasteners and, as such, is applied in this application by simulating both fastener lines as a single line with half the fastener distance. Further detail of this analysis approach is outlined in [23].

The figure displays 60 experimental data averages (five for each mode) and each is averaged from at least 25 tests. Some data averages from the early tests performed on configuration A are averaged from up to 100 tests. Therefore, Fig. 9 is constructed from a significant quantity of experimental data.

It can be seen from Fig. 9 that the riveted joint has consistently lower loss factor magnitudes than the equivalent bolted joint over the tested torque ranges. The bolt torque also is shown to have an effect on the loss factor magnitude. However, the relationship between the bolt torque and the loss factor is very dependent on mode shape. The data show that, as anticipated, cross and longitudinal bending modes

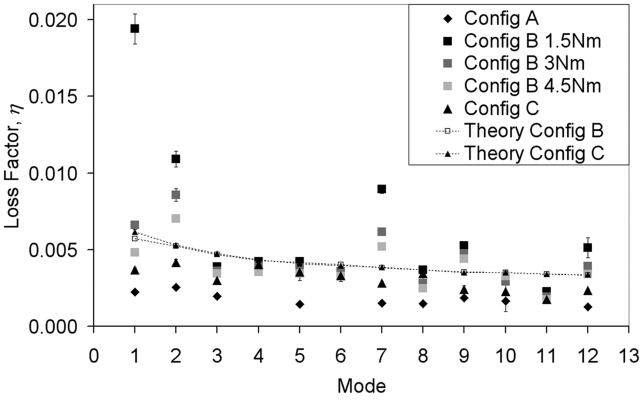

Fig. 9 Average experimental loss factors determined for five panel configurations.

are much more sensitive to a reduction in the joint stiffness. This is due to the fact that these mode shapes open the joint and therefore increase the effect of air pumping in the joint.

From a comparative inspection of the theoretical data in Fig. 9, it can be seen that, in general, the theoretical results give a good conservative estimate of the stiffer joint experimental results, considering the very low damping magnitudes. As the stiffness of the joint reduces, the model remains a good approximation for the mode shapes that are not sensitive to a stiffness reduction, i.e., the mode shapes that are not opening the joint and increasing the effect of air pumping.

To discuss the linearity of the experimental data, it is first necessary to identify how to present these data, as it is not practically possible to present 1500 different curves. It is not possible to average the curves, as this could remove the trends that need to be observed. Ten sample decay curves from each set of repeats (taken equally from all the tested accelerometer locations) were therefore processed and plotted together to select a representative decay curve for comparison with the decay curves of the other configurations. An example of this is shown in Fig. 10, where 10 decay curves are plotted for configuration B, 3 N · m, mode 7. It can be seen that all the trends are highly repeatable and the selection of one representative curve for further comparisons is shown to be valid. Any significant variation in these 10 sample decay curves will be noted and taken into account for the next stage of comparisons.

The selected representative curves for the different configurations are plotted together for each mode trend and can be seen in Figs. 11–14.

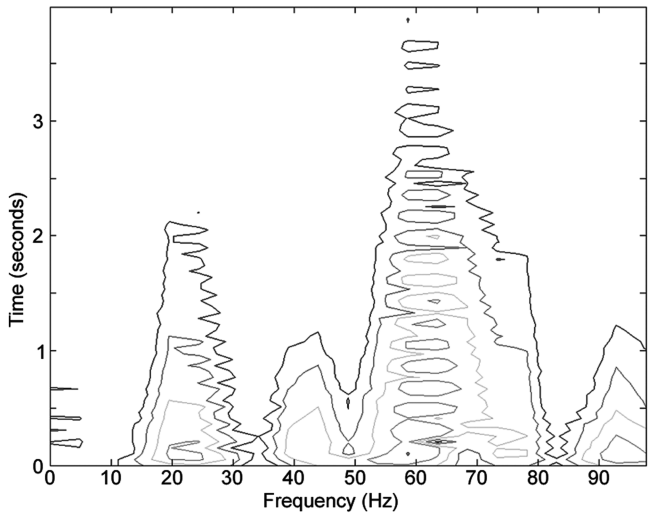

a)

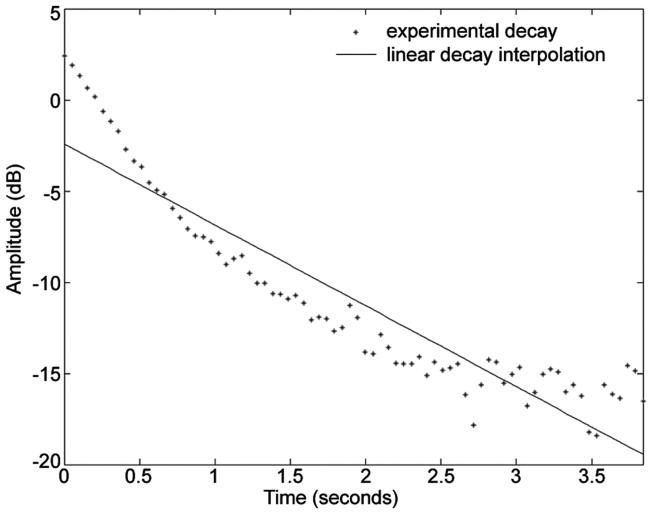

b)

Fig. 8 General output from sonogram analysis.

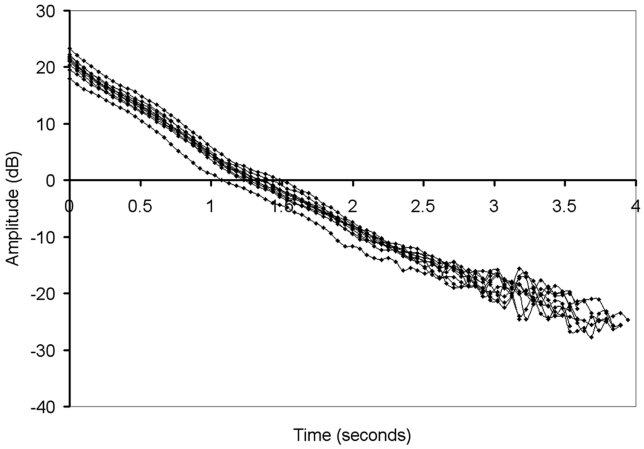

Fig. 10 Ten sample decay curves for configuration B, 3 N · m, mode 7.

Figure 11 displays all the representative decay data for the cross modes, i.e., modes 1, 7, 11, and 12. It is known from Fig. 9 that mode 1 has the largest variation in the damping magnitudes. This is clearly seen from the gradients in Fig. 11a. However, the nonlinearity of the decibel decay increases as the stiffness of the joint decreases. For the weakest bolted joint, the vibration amplitude follows more of an exponential decay trend. As the joint stiffness is increased, the nonlinearity reduces, resulting in a linear trend for the riveted joint with respect to the decibel reduction over time. For the higher modes, these nonlinearities are less apparent. Mode 7, although displaying the same gradient trends (a reduction in the damping as the joint stiffness increases), shows much more linear trends in the decibel decay rate. A similar distribution of the data is shown for mode 12. However, oscillations can be seen in the decay. The amplitude of these oscillations increases as the joint stiffness increases. The frequency of the oscillation also varies for each joint type. As these oscillations are seen for the monolithic panel in all the 10 sample decay curves, they cannot be ascribed with any certainty to an effect of the joint. They are far more likely to be caused by insufficient frequency resolution resulting from two modes being sufficiently close in frequency that they are not resolved by the short fast Fourier transforms of the sonogram. Every effort was taken to minimize the excitation of two modes at a similar frequency but, in practice, this is very hard to achieve. The data for mode 11 display a certain level of variability in data consistency not seen for the other modes. Although the representative data shown in Fig. 11c accurately display the decay gradients, inconsistent fluctuations were seen over the repeat tests, as shown in Fig. 15. This can be ascribed to varying degrees of frequency resolution at different accelerometer locations.

Although these inconsistencies were found, it can be seen that the overall decay rates are pretty consistent for all the configurations. This is due to the location of the joint for this particular mode shape. With the exception of mode 11, these cross modes display a variability of the damping with respect to the mode shape, and obvious nonlinearities with respect to the decibel reduction over time are only seen for mode 1.

The decay data for the longitudinal bending modes are displayed in Fig. 12, and it can be seen from Fig. 12a that, although the decibel

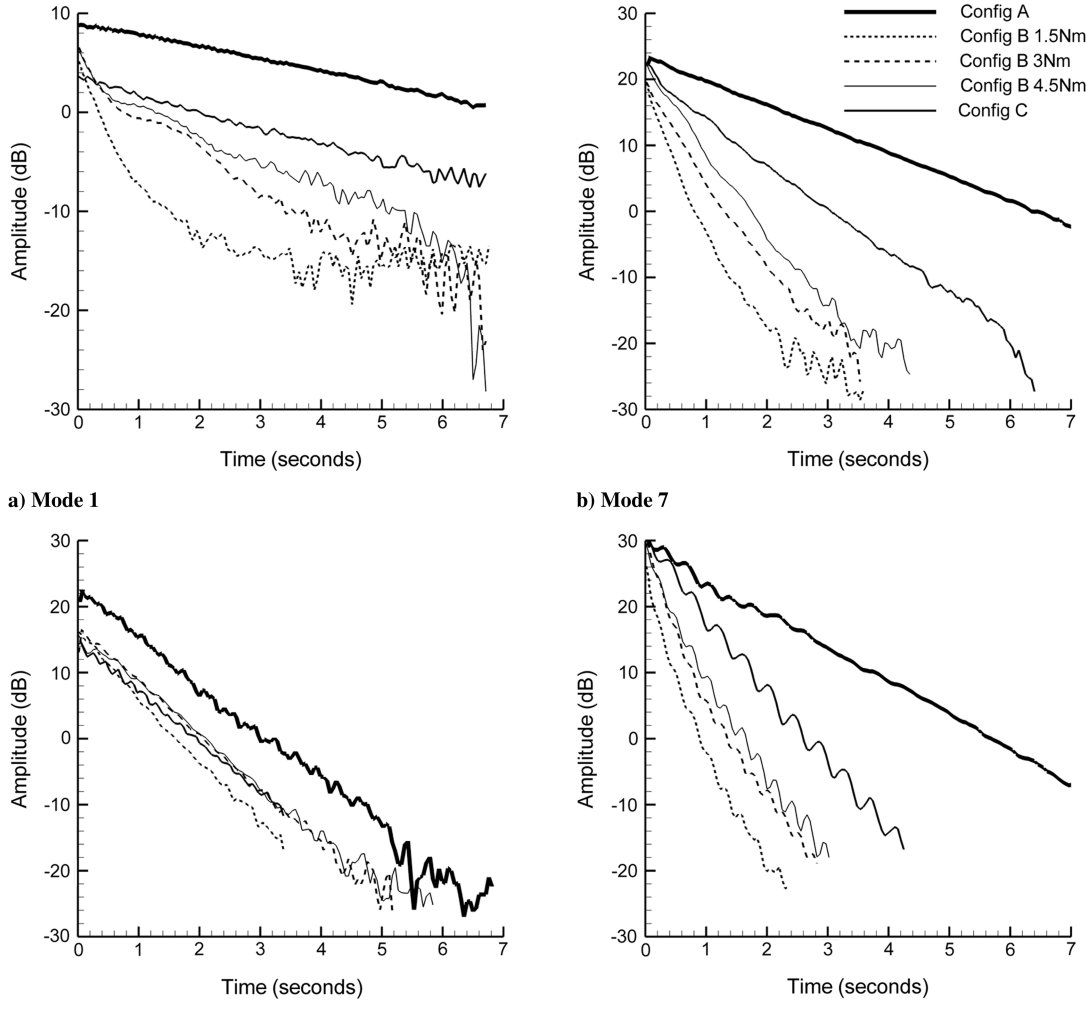

a) Mode 1 **b) Mode 7**

c) Mode 11 **d) Mode 12**

Fig. 11 Decay rates for cross modes (1, 7, 11, 12).

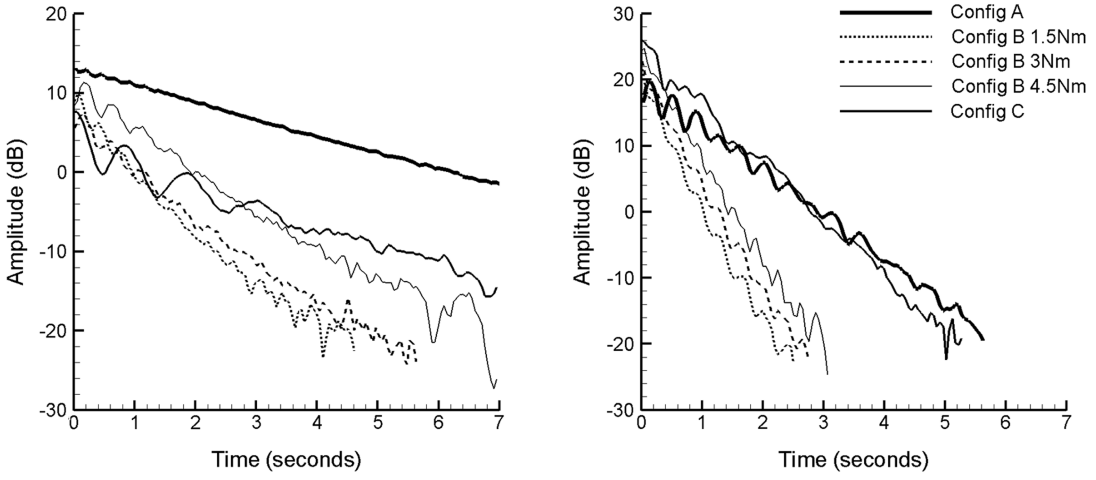

a) Mode 2 b) Mode 9

Fig. 12 Decay rates for longitudinal bending modes (2, 9).

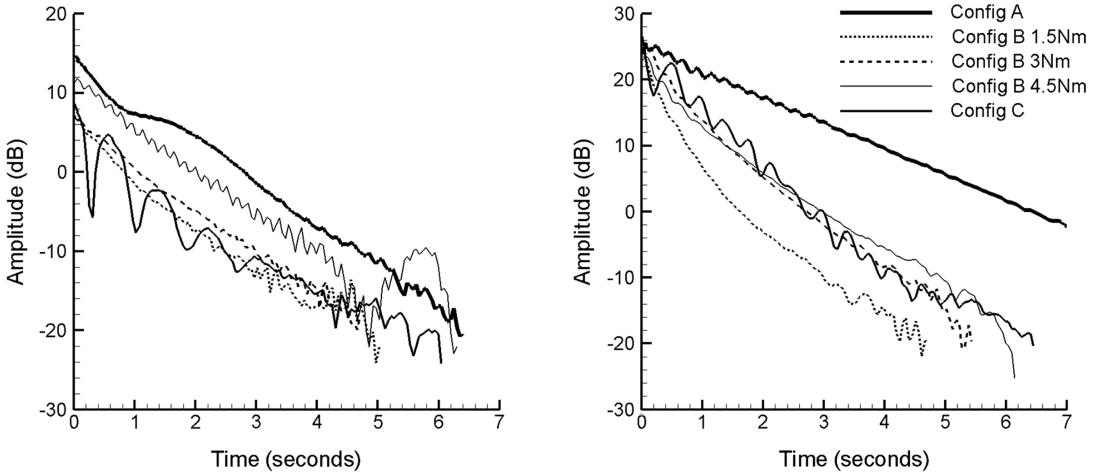

a) Mode 4 b) Mode 8

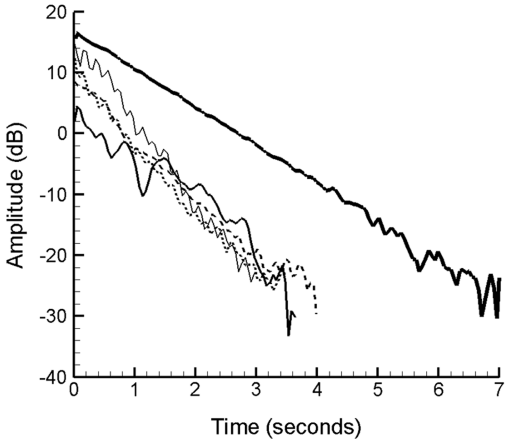

c) Mode 10

Fig. 13 Decay rates for transverse bending modes (4, 8, 10).

decay of configuration A is linear, small oscillation amplitudes increase as the stiffness of the joint increases. The lower stiffness joints display a slightly nonlinear decibel decay curve but not as apparent as for mode 1. The decay rates for mode 9 follow a similar pattern to mode 12. Small oscillations are seen for all configurations; however, the decay gradients are consistent.

The decay data for the transverse bending modes are shown in Fig. 13. Although small nonlinearities with respect to the decibel reduction over time can be seen for configuration A, the riveted joint displays consistent nonrepeating nonlinearities for all three mode shapes. Minor effects are also noted for the tightest bolted joint and these fluctuations tend to reduce as the bolt torque reduces. The randomness of these decays suggests that these oscillations are proportional to the clamping strength of the joint and therefore could be ascribed to friction in the joint. Such properties are also seen for mode 2 and therefore similar suggestions could be made for this

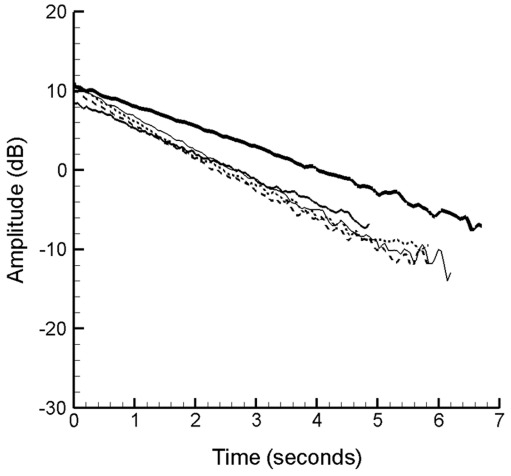

a) Mode 3

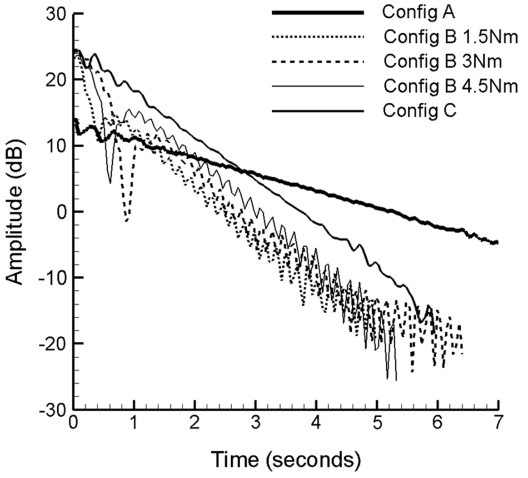

b) Mode 5

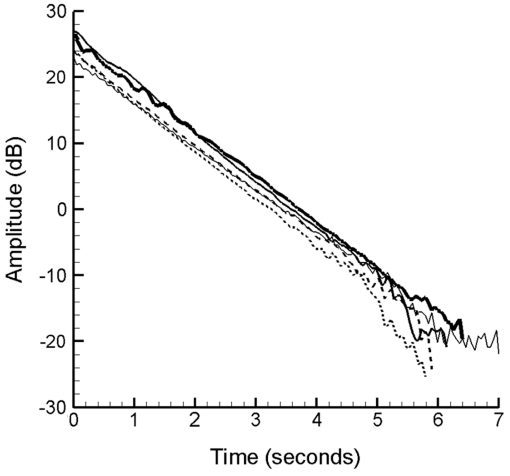

c) Mode 6

Fig. 14 Decay rates for variable modes (3, 5, 6).

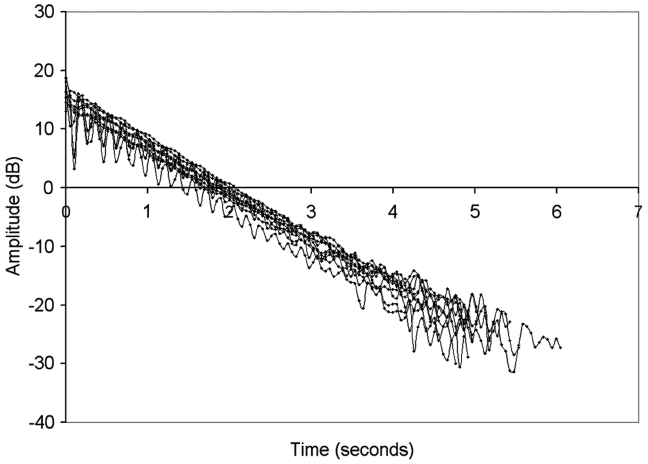

Fig. 15 All decay curves for configuration B, 3 N · m, mode 11.

mode shape. It should also be noted that configurations B, 1.5 and 3 N · m in Fig. 13, display a curving decibel decay rate highlighting the potential nonlinearity with respect to the decibel reduction over time of these mode shapes.

The decay rates for the variable mode shape group can be seen in Fig. 14. The first obvious trend is that the decibel decay rates for both modes 3 and 6 are very linear, with only minor fluctuations between the gradients for the different configurations. This is because the mode shapes do not tend to excite the location of the joint as shown in Fig. 3. Therefore, there is little impact from friction or air pumping in the joint. Mode 5, however, displays irregular repeatable characteristics for configuration B. A dip in the decay rate can be seen, leading to an oscillatory decay of the vibration. The source of this is unknown and it may well be the influence of an external effect, as the mode shape does not suggest that any irregularity should be caused. Such trends are not seen for configuration C, even though the decay gradients are very similar.

VI. Conclusions

This publication has experimentally investigated the damping linearity and magnitude of bolted and riveted aluminium panels using a test method that minimizes any external influences on the natural free vibration of the panel. The experimental damping magnitudes have been compared with the theoretical model outlined by Ungar [22] and were classified by the displacement trends of the joint edges into cross, longitudinal bending, transverse bending, and variable modes. It can be concluded that

1) Ungar's model is a good conservative estimate of the damping magnitudes for the higher stiffness joints over all the first 12 modes.

2) The largest damping magnitudes occur for mode shapes that open up the joint and, consequentially, increases the effect of air pumping.

3) Nonlinearity decays of the logarithmic damping over time occur for the low stiffness joints and are most apparent for mode shapes 1, 2, 4, and 8.

4) The nonlinearities for the transverse bending modes were the result of frictional effects due to the random nature of the oscillations in the decay rate.

5) Some of the variable mode shapes only have a very minor contribution to the damping of the panel, as the location of the joint is not excited.

6) In general, the majority of logarithmic decays do follow an overall linear trend, however, care must be taken when using linear interpolations for low stiffness joints.

The combination of the damping behavior from all the modes creates the damping parameter for the complete structure. If the way the location of the joint is displaced for each mode shape governs the dominant damping mechanism for each mode, then the final damping parameter will be a combination these factors, namely, friction, air pumping, etc. It can therefore be concluded that to determine the detailed proportional difference of these effects, it would be necessary to study the mode shapes in more detail; for example, study the modal damping values of the cross and longitudinal bending modes at various air pressures and the effects of friction on the transverse bending modes. However, the general conclusion from the average loss factor magnitude data and the comparison of the theoretical model is that, for these panels, air pumping is the largest single damping contribution.

References

[1] Ungar, E., *Noise and Vibration Control Engineering: Principles and Applications*, Wiley, New York, 1992, ISBN 0-471-61751-2.

[2] Phani, S. A., "Damping Identification in Linear Vibration," Ph.D. Thesis, St. John's College, Cambridge, England, U.K., Jan. 2004.

[3] Salzmann, A., Fragomeni, S., and Loo, Y., "Damping Analysis of Concrete Beams Under Free Vibration," *Advances in Structural Engineering*, Vol. 6, No. 1, 2003, pp. 53–64. doi:10.1260/136943303321625739

[4] Gibson, R. F., "Nontraditional Application of Damping Measurements," *Symposium on M3D: Mechanics and Mechanisms of Material Damping*, American Society for Testing and Materials, No. 1169, 1992, pp. 60–75.

[5] Earles, S., "Theoretical Estimation of the Frictional Energy Dissipation in a Simple Lap Joint," *Journal of Mechanical Engineering Science*, Vol. 8, No. 2, 1966, pp. 207–214. doi:10.1243/JMES_JOUR_1966_008_025_02

[6] Maidanik, G., "Energy Dissipation Associated with Gas Pumping in Structural Joints," *Journal of the Acoustical Society of America*, Vol. 40, No. 5, 1966, pp. 1064–1072. doi:10.1121/1.1910189

[7] Feng, L., "Vibration Insertion Loss of Traditional and Smart Joints," *Acta Acustica*, Vol. 87, No. 2, 2001, pp. 199–205.

[8] Walker, S. J. I., Aglietti, G. S., and Cunningham, P. R., "Study of Joint Damping in Metal Plates," *Proceedings of the 57th International Astronautical Congress*, International Astronautical Congress IAC-06-C2.3.10, 2006.

[9] Mead, D. J., "Structural Damping and Damped Vibration," *Applied Mechanics Reviews*, Vol. 55, No. 6, 2002, pp. R45–R54. doi:10.1115/1.1495523

[10] Wylie, A., Vibration Damping in Structural Joints, 4th Year Project, Univ. of Cambridge, Cambridge, England, U.K., 1997–1998.

[11] Jarvis, B. P., "Simple Joint Models," *Proceedings of the ISMA 25, International Conference on Noise and Vibration Engineering*, Vol. 2, 2000, pp. 801–805.

[12] Moloney, C. W., Peairs, D. M., and Roldan, E. R., "Characterization of Damping in Bolted Lap Joints," *Proceedings of IMAX-XIX: A Conference on Structural Dynamics*, 2001.

[13] Esteban, J., and Rogers, C. A., "Energy Dissipation Through Joints: Theory and Experiments," *Computers and Structures*, Vol. 75, No. 4, 2000, pp. 347–359. doi:10.1016/S0045-7949(99)00096-6

[14] Gaul, L., and Lenz, J., "Nonlinear Dynamics of Structures Assembled by Bolted Joints," *Acta Mechanica*, Vol. 125, Nos. 1–4, 1997, pp. 169–181. doi:10.1007/BF01177306

[15] Tsai, J. S., and Chou, Y. F., "Identification of Dynamic Characteristics of a Single Bolt Joint," *Journal of Sound and Vibration*, Vol. 125, No. 3, 1988, pp. 487–502. doi:10.1016/0022-460X(88)90256-8

[16] Scott, J. E., and Orabi, I. I., "Prediction and Measurement of Joint Damping in Scaled Model Space Structures," *Proceedings of the Fourteenth Engineering Mechanics Conference*, 2000.

[17] Deraemaeker, A., Ladeveze, P., Collard, E., and Leconte, P., "Modeling and Identification of Joint Parameters: Application to Bolted Plates," *Proceedings of the ISMA 25*, Vol. 2, 2000, pp. 785–791.

[18] Hodges, C., Power, J., and Woodhouse, J., "Use of the Sonogram in Structural Acoustics and an Application to the Vibrations of Cylindrical Shells," *Journal of Sound and Vibration*, Vol. 101, No. 2, 1985, pp. 203–218.

[19] Hays, S., *Outline of Statistics*, 6th ed., Longmans, Harlow, Essex, U.K., 1962.

[20] Walker, S. J. I., Aglietti, G. S., and Cunningham, P. R., "Experimental Analysis of Damping Across Joints in Metal Plates," *Applied Mechanics and Materials*, Vols. 5–6, Sept. 2006, pp. 391–398.

[21] Moaveni, S., *Finite Element Analysis: Theory and Application with ANSYS*, Prentice–Hall, Upper Saddle River, NJ, 1999, ISBN: 0137850980.

[22] Ungar, E. E., "Damping of Panels Due to Ambient Air," *Damping Applications in Vibration Control*, edited by P. J. Torvik, AMD-Vol. 38, American Society of Mechanical Engineers, New York, 1980, pp. 73–81.

[23] Walker, S. J. I., Aglietti, G. S., and Cunningham, P. R., "Low Frequency Damping of Metal Panels in Ambient Air," *Journal of Mechanical Engineering Science* (to be published), 2008.

J. Wei
Associate Editor